

Stochastic aspects of thermoacoustic instabilities in combustion chambers

Conference Paper

Author(s):

Noiray, Nicolas; Denisov, Alexey

Publication date:

2016

Permanent link:

<https://doi.org/10.3929/ethz-a-010819429>

Rights / license:

[In Copyright - Non-Commercial Use Permitted](#)

Stochastic aspects of thermoacoustic instabilities in combustion chambers

Nicolas Noiray*¹ and Alexey Denisov²

¹CAPS Lab., Mechanical and Process Engineering Dep., ETH Zürich, Switzerland

²Paul Scherrer Institute, Villigen, Switzerland

Summary The stochastic nature of combustion instabilities in practical land-based gas turbines and aeroengines combustors has seldom been investigated. It is shown here that a wealth of information about the constructive acoustic-flame interactions can be gained by scrutinizing the effects of the inherent turbulence-induced noise which forces the nonlinear thermoacoustic dynamics. In particular, one presents a method, based on the Fokker-Planck formalism, to identify from dynamic pressure signals the linear growth rates, the type of flame response nonlinearity and the potential defining the system acoustic energy. It is applied to and validated against experimental data measured in a lab-scale combustion chamber.

Due to the lack of cost-effective actuators, passive damping technologies constitute the vast majority of thermoacoustic instability control systems in practical combustors. It has been shown that robust design of these dampers requires the knowledge of the thermoacoustic linear growth rates [1]. Up to now, only linear decay rates providing stability margin could be quantified, because common output-only system identification (SI) methods used to process pressure data necessitate linearly stable system. Recently, it has been shown that one can take advantage of the presence of inherent turbulent combustion noise to extract linear growth rates from limit cycle data [2, 3]. This SI is based on the work of Friedrich and co-workers [4].

A cylindrical combustion chamber operated at atmospheric pressure is used. The thermal power is approximately 30 kW. The turbulent swirled V-flame is anchored at the rim of a lance equipped with an axial swirler. The acoustic pressure in the combustion chamber is measured by using a calibrated water-cooled microphone. When the equivalence ratio is varied from 0.47 to 0.5 by increasing the fuel mass flow, the acoustic level in the combustion chamber sharply increases due to the constructive interaction between the flame and one of the longitudinal acoustic modes (Fig. 1a). At condition c_3 , the acoustic pressure probability density function $P(p)$ exhibits a bimodal distribution, which is typical of stochastic limit cycle oscillation. In contrast, at condition c_1 , the PDF has a gaussian like distribution which is characteristic of randomly excited linearly stable oscillator. High speed Particle Image Velocimetry is performed at condition c_3 and proper orthogonal decomposition (POD) is computed from 2 seconds data (see Fig. 1b and 1c). The first two POD modes, exhibiting an axially shifted pattern of coherent structures typical of coherent vortex shedding and advection, carry nearly 20 % of the kinetic energy. The corresponding axisymmetric roll-up of vortices from the burner exit occurs at the thermoacoustic mode frequency around 150 Hz.

Starting from the acoustic wave equation with heat release rate source term, one can derive a Langevin equation for the acoustic pressure envelope $A(t)$, where the acoustic pressure is defined by $p = A(t) \cos(\omega t + \phi(t))$. This derivation is based on the following assumptions, which are valid for many practical situations: (i) a single thermoacoustic mode resulting from the constructive acoustic-flame interaction dictates the flow dynamics, (ii) the flame heat-release-rate fluctuations can be decomposed into a coherent and a noisy part $\hat{q} = \hat{q}_c + \hat{q}_n$, the former resulting from the acoustically driven heat release rate fluctuations and the latter from the intense turbulence pertaining to practical combustion chambers, (iii) the coherent flame response to acoustic perturbations exhibits a sigmoid type saturation when the acoustic level increases, which is approximated

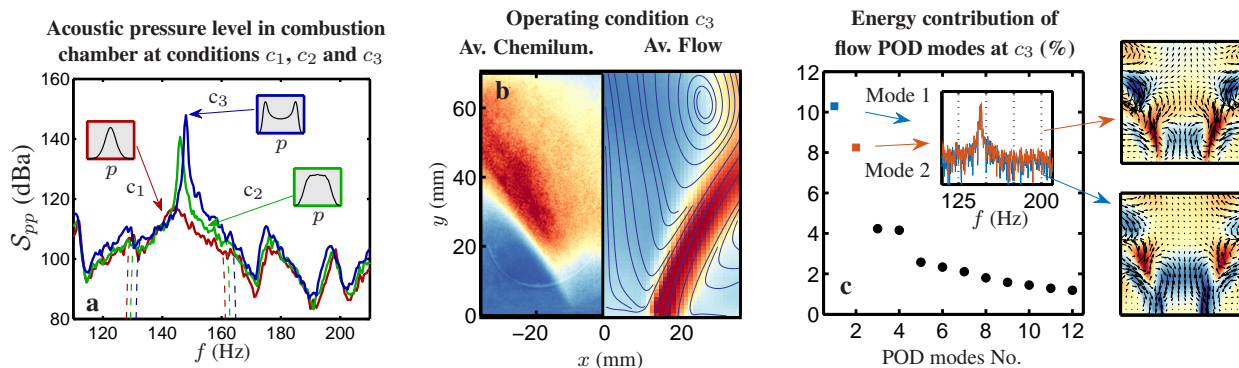


Fig. 1: (a) Acoustic power spectral density from signals measured in the atmospheric-pressure combustion chamber at different equivalence ratios (≈ 30 kW thermal power), and corresponding acoustic pressure probability density functions P_p . (b) Averaged OH* chemiluminescence from the turbulent V flame, and averaged axial velocity field from -8 (blue) to 15 m/s (red) at self-oscillating condition c_3 . (c) Energy contribution of the first 12 POD modes deduced from 2 seconds data (294 acoustic cycles) at condition c_3 , and POD modes 1 and 2 (blue and red for negative and positive axial displacement). Also shown, the Fourier transforms of the POD modes amplitudes.

*Corresponding author. Email: noirayn@ethz.ch

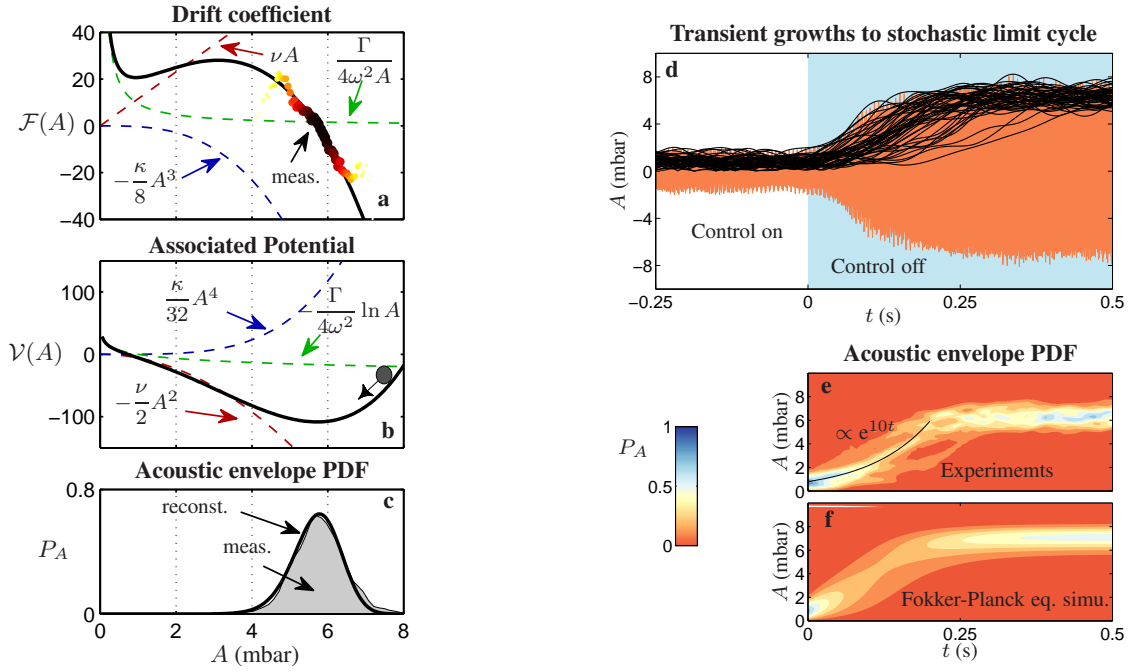


Fig. 2: Processing of the statistics of the acoustic pressure envelope A at operating condition c_3 . **(a)** 1st transition moment of the amplitude A processed from the envelope of the 30 seconds limit-cycle acoustic pressure data (symbols coloured by P_A) and corresponding best fit (thick line). The parameters Γ , ν and κ are optimised using the assumed theoretical model. Also included as thin dotted lines the identified linear, nonlinear and stochastic contributions. **(b)** Potential defining the system acoustic energy deduced from the output-only system identification process. **(c)** PDF reconstructed from the identification process using theoretical model superimposed on the one directly computed from the acoustic signal. **(d)** 100 superimposed transient growths around control-switch-off instants for conditions c_3 . **(e)** corresponding PDF. **(f)** Simulation of the Fokker-Planck equation (1) using the parameters obtained from the output-only SI method, with initial condition taken from the experimental PDF shown at $t = 0$ in (e).

by a cubic type nonlinearity $q_c = \beta\eta - \kappa/3\eta^3$ on a range of acoustic amplitudes, where η is the acoustic mode amplitude. In the ideal deterministic case, when the source term β exceeds the mode linear damping α , it yields an exponential amplification of perturbations at a growth rate $\nu = (\beta - \alpha)/2$. The resulting Langevin equation with additive forcing ζ of intensity $\Gamma/2\omega^2$ and the associated Fokker-Planck equation describing the evolution of the probability $P(A, t)$ are given below:

$$\dot{A} = -\frac{\partial \mathcal{V}}{\partial A} + \zeta, \quad \text{and} \quad \frac{\partial}{\partial t} P_{A,t} = -\frac{\partial}{\partial A} (\mathcal{F}(A) P_{A,t}) + \frac{\Gamma}{4\omega^2} \frac{\partial^2}{\partial A^2} P_{A,t}, \quad (1)$$

where the potential $\mathcal{V}(A) = \nu/2 A^2 + \kappa/32 A^4 - \Gamma/4\omega^2 \ln A$, is linked to the drift coefficient as $\mathcal{F}(A) = -\partial \mathcal{V}/\partial A$. The potential defines the acoustic energy of the system because for standing oscillations, the latter is proportional to the square of the acoustic pressure envelope A measured at a given location. Considering that $\mathcal{F}(A) = \lim_{\tau \rightarrow 0} \frac{1}{\tau} \int_{-\infty}^{\infty} (a - A) P_{A|a}^{\tau} da$, one computes the drift coefficient by acoustic-pressure-records binning, and subsequently perform model-based fit to extract the governing parameters, especially the linear growth rate ν (see Fig. 2a-c). The results from this SI approach are then validated using an active control system allowing us to periodically trigger transient growths to the stationary stochastic limit cycle. The Fokker-Planck equation fed with the identified parameters is numerically integrated and one can see in Fig. 2d-f that the simulation results are in remarkable agreement with the measured ones, which validates the SI method.

This methodology constitutes a significant step forward for practical applications, because it can be applied to validate low-order thermoacoustic network models used for stability analysis, and also to reliably design effective damping systems.

References

- [1] N. Noiray and B. Schuermans. Theoretical and experimental investigations on damper performance for suppression of thermoacoustic oscillations. *Journal of sound and vibration*, 331(12):2753–2763, 2012.
- [2] N. Noiray and B. Schuermans. Deterministic quantities characterizing noise driven hopf bifurcations in gas turbine combustor. *Int. J. Non-linear Mechanics*, 50:152–163, 2013.
- [3] N. Noiray and B. Schuermans. On the dynamic nature of azimuthal thermoacoustic modes in annular gas turbine combustion chambers. *Proc. Roy. Soc. A*, 469(20120535), 2013.
- [4] R. Friedrich, J. Peinke, M Sahimi, and M. R. R. Tabar. Approaching complexity by stochastic methods: From biological systems to turbulence. *Phys. Reports*, 506:87–162, 2011.